Cell Reports, Volume *23*

Supplemental Information

A Multi-layered Quantitative *In Vivo* Expression Atlas of the Podocyte Unravels Kidney Disease Candidate Genes

Markus M. Rinschen, Markus Gödel, Florian Grahammer, Stefan Zschiedrich, Martin Helmstädter, Oliver Kretz, Mostafa Zarei, Daniela A. Braun, Sebastian Dittrich, Caroline Pahmeyer, Patricia Schroder, Carolin Teetzen, HeonYung Gee, Ghaleb Daouk, Martin Pohl, Elisa Kuhn, Bernhard Schermer, Victoria Küttner, Melanie Boerries, Hauke Busch, Mario Schiffer, Carsten Bergmann, Marcus Krüger, Friedhelm Hildebrandt, Joern Dengjel, Thomas Benzing, and Tobias B. Huber

A

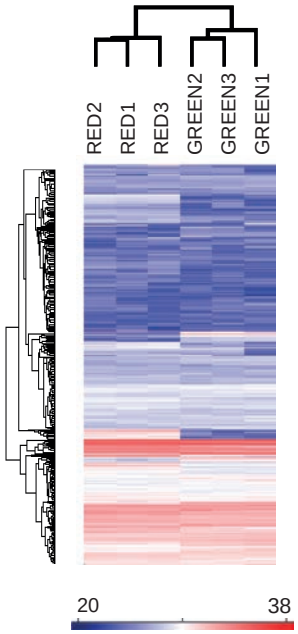
RED2
RED1
RED3
GREEN2
GREEN3
GREEN1
20
38

B

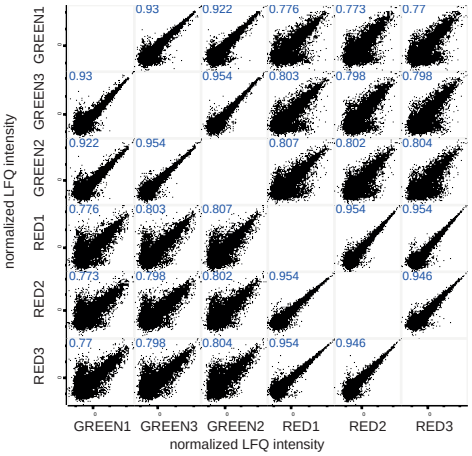
GREEN1
GREEN3
GREEN2
RED1
RED2
RED3
0.93
0.922
0.776
0.773
0.77
0.954
0.803
0.798
0.807
0.802
0.804
0.954
0.946
normalized LFQ intensity
normalized LFQ intensity

C

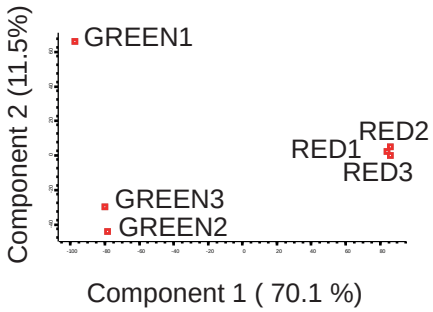
GREEN1
RED2
RED1
RED3
GREEN3
GREEN2
Component 2 (11.5%)
Component 1 (70.1 %)

Fig. S1

Fig. S1. Quality controls of the proteomic dataset, Related to Fig. 1. A. Analysis of lable-free quantitative intensities reveals a strong separation between podocytes (green) and non-podocytes (red) quantitative proteome profiles. B. Multi scatter plots of LFQ intensities indicate a clear separation between podocytes (green) and non-podocytes (red) and a high correlation between biological replicates. Pearson's correlation coefficients are annotated. C. Principal component analysis of protein expression values of samples in this study.

A

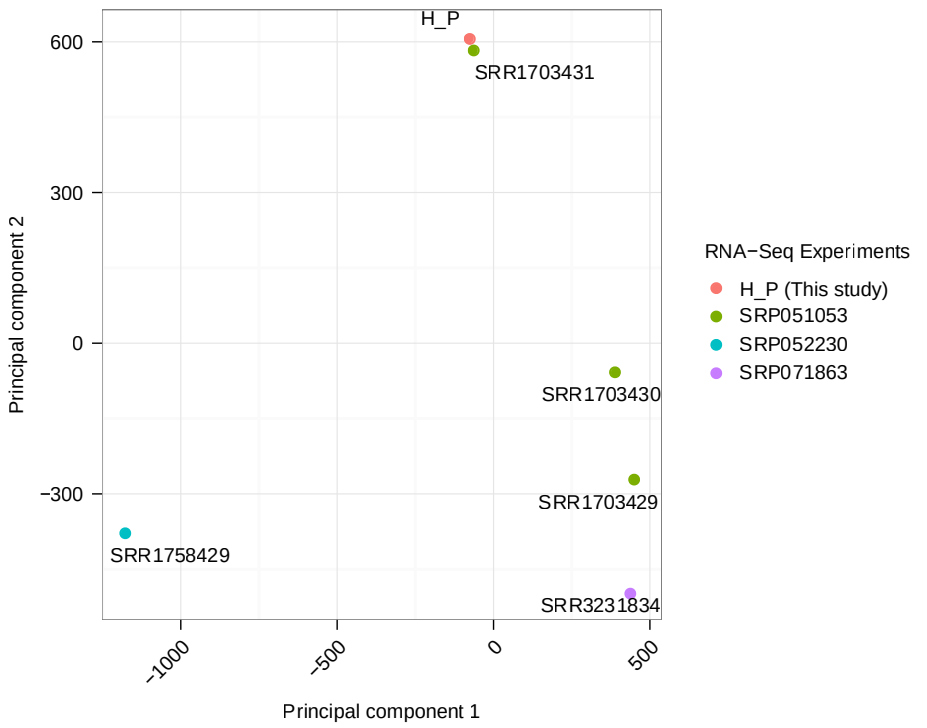

B

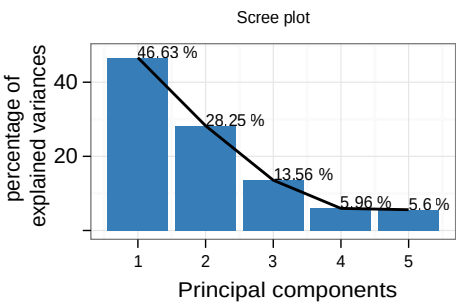

C

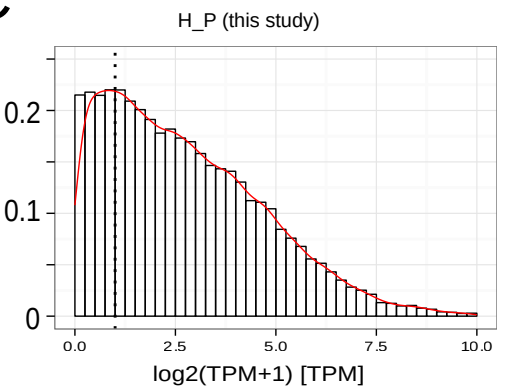

D

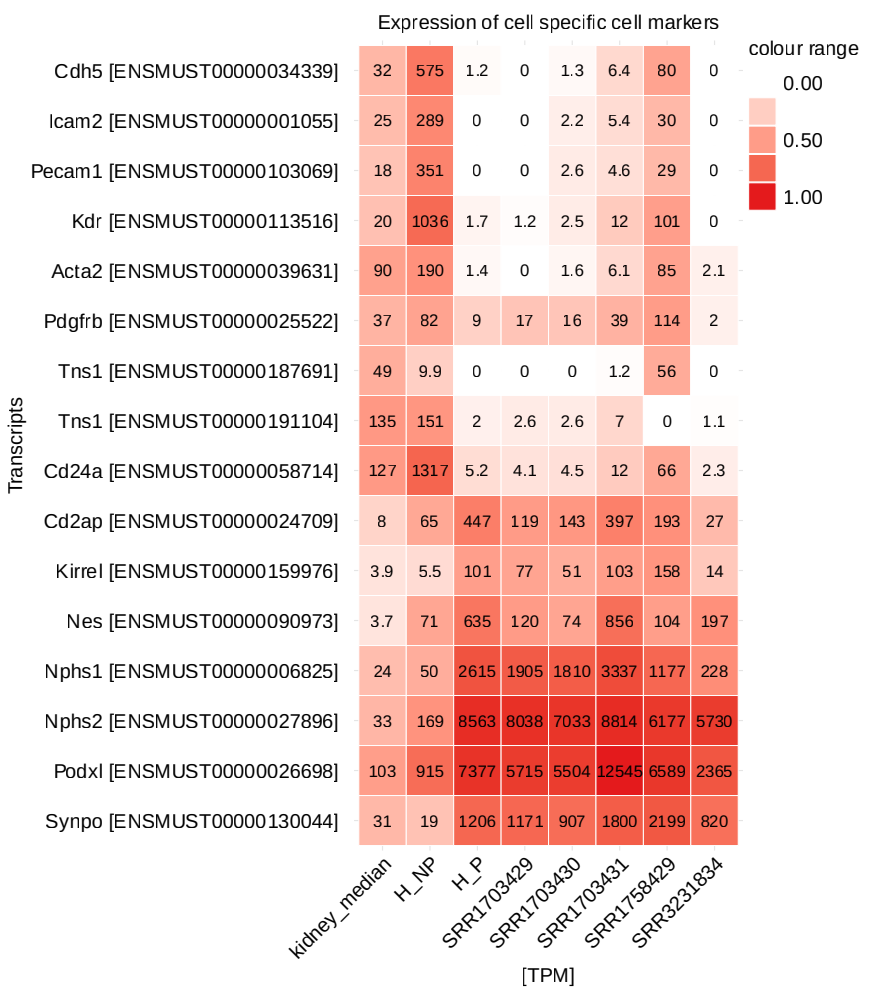

E

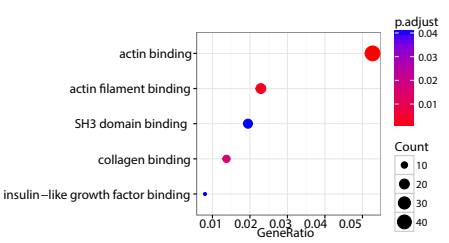

F

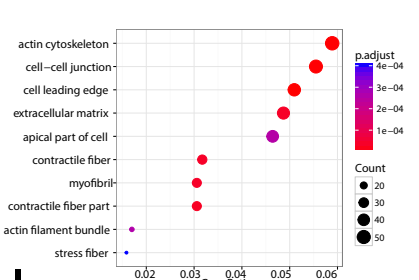

G

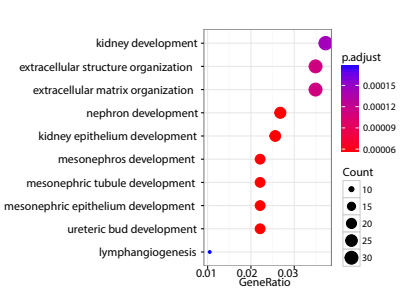

H

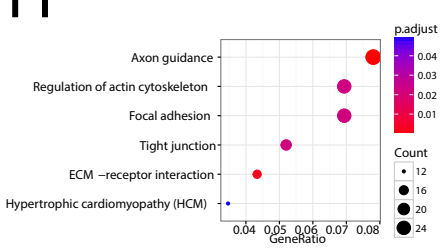

I

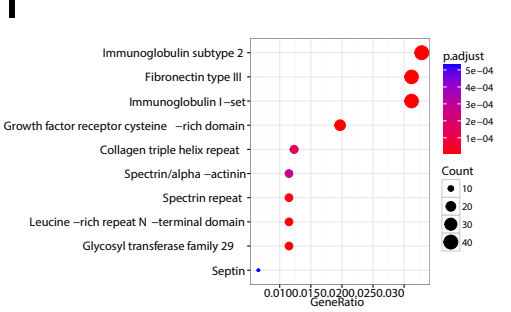

Fig. S2

Fig. S2. Transcriptome quality controls and overexpressed gene sets, Related to Fig. 2. A. PCA analysis of published podocyte mRNA-Seq studies (see Table S3 for details, H_P is our study). B. Contribution to principal components. C. Histogramm and density plot of tpm values from our podocyte mRNA-Seq study. D. Comparison of tpm values of podocyte, mesangial cell and endothelial cell marker genes. Our Podocyte RNA-Seq study as well as the studies of Kann et al.(6) and Fu et al. (8) proofed to be podocyte specific with only minimal expression of mesangial and endothelial marker genes (H_NP is our RNA-Seq study on non-podocyte glomerular cells, H_P is our study on podocytes, see Table S3 for details of further studies). E-I. Overrepresented Genesets in podocyte compared to non-podocyte glomerular cells transcriptomes. Related to Fig. 2. E. GO molecular function. F. GO cellular component. G. GO biological process. H. KEGG-pathway. I. Interpro domains

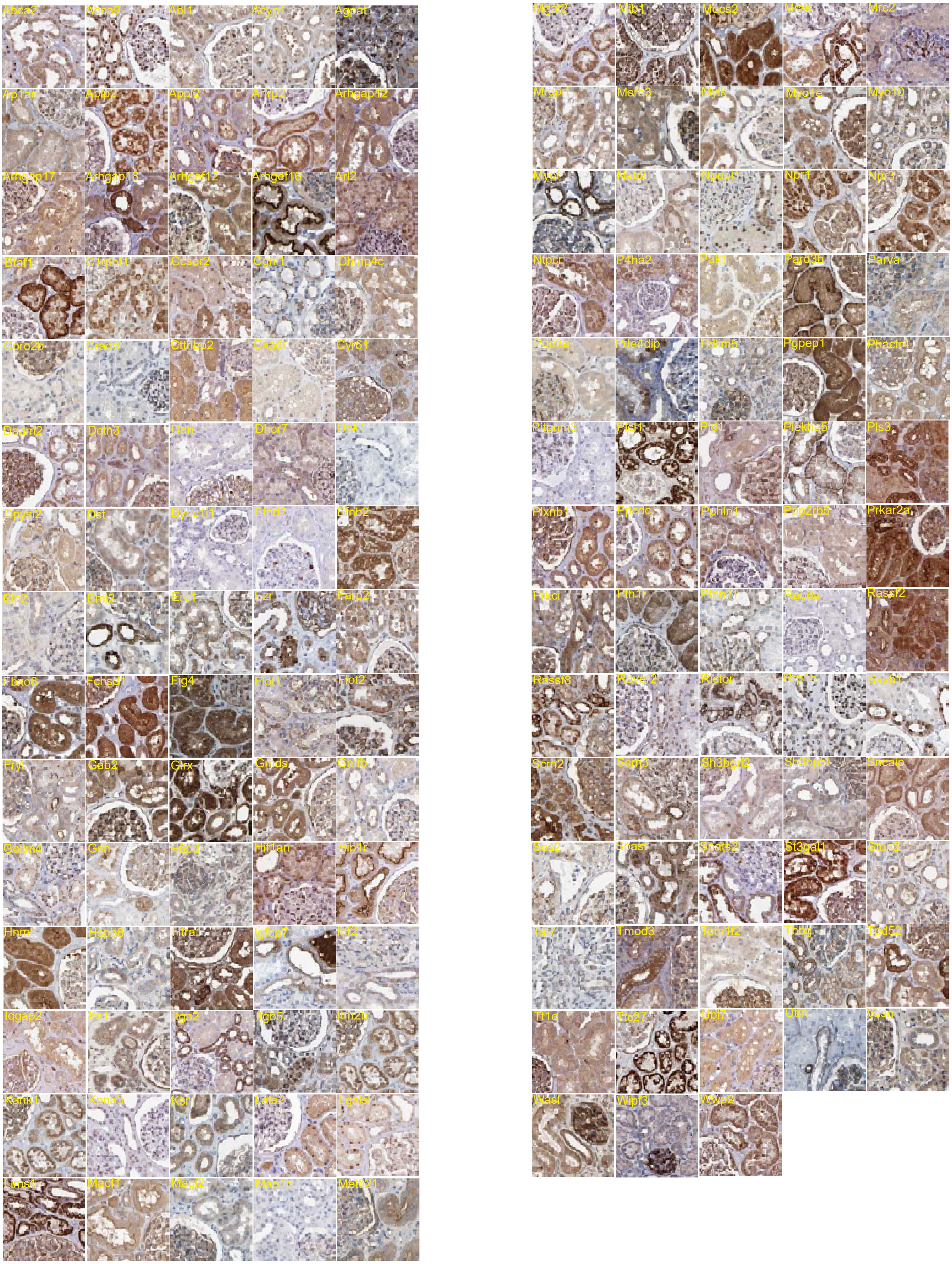

Abca2
Abca9
Abl1
Acyp1
Agpat
Ap1ar
Aplp2
Appl2
Arfrp2
Arhgap12
Arhgap17
Arhgap18
Arhgef12
Arhgef18
Arl2
Btaf1
C1qtnf1
Ccser2
Cgnl1
Chmp4c
Coro2b
Cradd
Cttnbp2
Cxadr
Cyr61
Daam2
Dctn3
Ddn
Dhcr7
Dok1
Dpysl2
Dst
Dync1i1
Efhd2
Efnb2
Elp2
Eml2
Erc1
Ezr
Farp2
Fbxo6
Fchsd1
Fig4
Flot1
Flot2
Fryl
Gab2
Glrx
Gmds
Gmfb
Golim4
Gsn
H6pd
Hif1an
Hip1r
Hnmt
Hspb8
Htra1
Igfbp7
Inf2
Iqgap2
Irs1
Itga2
Itgb5
Itm2b
Kank1
Kpna3
Krr1
Lats2
Lgalsl
Lims1
Macf1
Magi2
Map1b
Mettl21
Mgat2
Mib1
Mocs2
Mras
Mrc2
Mrgprf
Msrb3
Mylk
Myo1e
Myo10
Myof
Nab2
Npepl1
Npr1
Npr3
Ntpcr
P4ha2
Pak1
Pard3b
Parva
Pde3a
Pde4dip
Pdlim5
Pgpep1
Phactr4
Pitpnm3
Pls1
Pld1
Plekha5
Pls3
Plxnb1
Ppcdc
Pphln1
Ppp2r5b
Prkar2a
Prkci
Pth1r
Ptpn11
Rab6a
Rassf2
Rassf8
Raver2
Rictor
Rrp1b
Sash1
Scrn2
Scrn3
Sh3bgrl2
Sh3bp5l
Sncaip
Sos2
Spast
Spats2l
St3gal1
Ston2
Taf7
Tmod3
Tom1l2
Tpbg
Tpd52
Tt1c
Ttc27
Ubl7
Utrn
Vasn
Wasl
Wipf3
Wwp2

Fig. S3

Fig. S3: Glomerular staining of podocyte-enriched proteins in the human protein atlas. Related to Fig. 3. Proteins significantly enriched in podocytes were mapped on the human protein atlas (https://www.proteinatlas.org/). The figure shows proteins with “medium” protein staining in the resource. Corresponding mouse gene symbols are annotated.

A

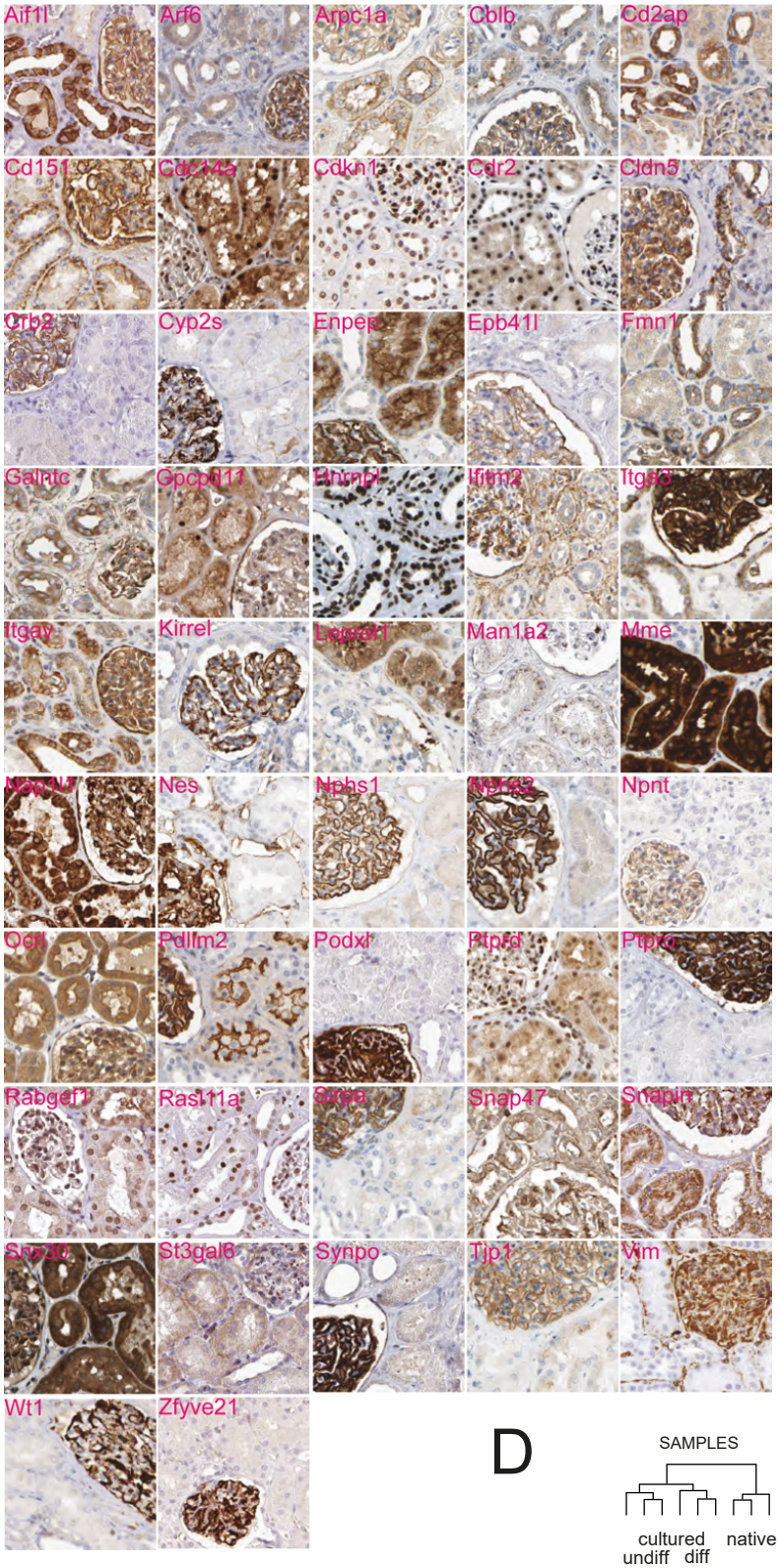
Aif1l
Arf6
Arpc1a
Cblb
Cd2ap
Cd151
Cdc42a
Cdkn1c
Cdr2
Cldn5
Crb2
Cyp2s
Enpep
Epb41l
Fmn1
Galntc
Gpcpd1
Hnrnpl
Ifitm2
Itga3
Itgav
Kirrel
Lasp1
Man1a2
Mme
Nap1l
Nes
Nphs1
Nphs2
Npnt
Qdpr
Pdlim2
Podxl
Ptpro
Ptprq
Rabgef1
Ras11a
Stbd1
Snap47
Snapin
Snx30
St3gal6
Synpo
Tjp1
Vim
Wt1
Zfyve21

B

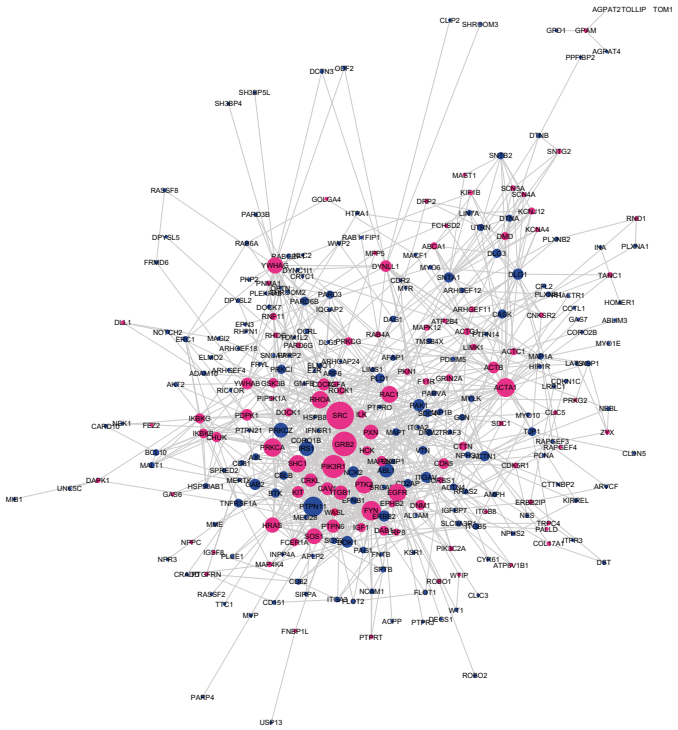

C

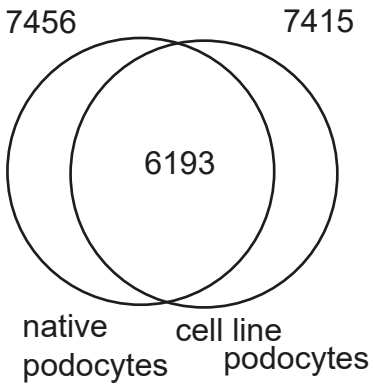
7456
7415
6193
native podocytes
cell line podocytes

D

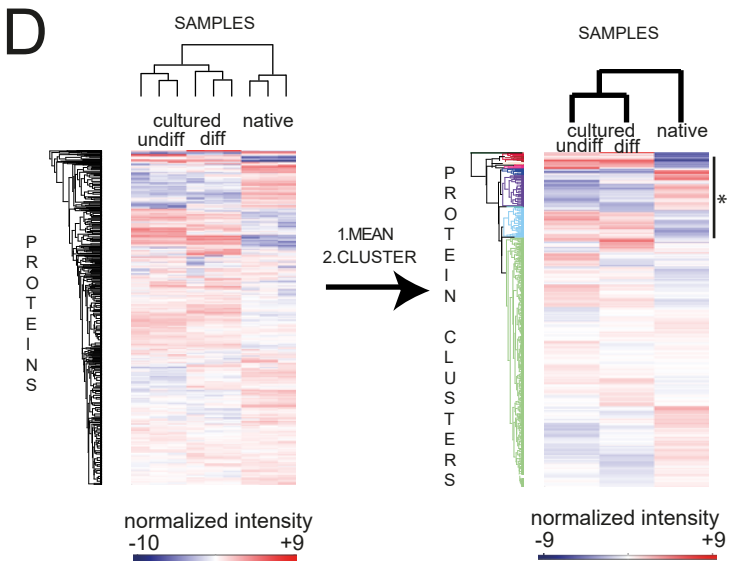
SAMPLES
cultured undiff
diff
native
PROTEINS
normalized intensity
-10
+9
1.MEAN
2.CLUSTER
SAMPLES
cultured undiff
diff
native
PROTEIN CLUSTERS
*
normalized intensity
-9
+9

Fig. S4

Fig. S4. Glomerular staining of podocyte-enriched proteins in the human protein atlas, podocyte-specific interaction network and comparison between cultured and native podocytes, Related to Fig. 3 and 4. A: Proteins significantly enriched in podocytes were mapped on the human protein atlas (https://www.proteinatlas.org/). The figure shows proteins with “strong” protein staining in the resource. Gene symbols are annotated. B. Podocyte-enriched interaction network. Podocyte-enriched proteins (n=541) were analyzed with the Netbox software for common interactors (p-value threshold $p<0.05$). Nodes represent proteins, whereas edges represent interactions. Proteins in the initial dataset of podocyte-specific proteins are depicted in blue, whereas proteins determined as “linker” proteins (not in the initial datasets) are depicted in magenta. The node size is proportional to the number of interactions. Src is a major node in the podocyte-specific interaction network. C-D. Comparison of cultured and native podocyte proteome. Overlap between this dataset and samples from cultured mouse podocytes (33°C, undifferentiated and 37°C, differentiated, samples previously published [Rinschen et al. AJP cell 2016, DOI:10.1152/ajpcell.00121.2016]) were compared. D. Intensities of the common proteins between the podocyte proteome and the previously acquired podocyte proteome were normalized and clustered using hierarchical clustering. 8 major clusters were defined.

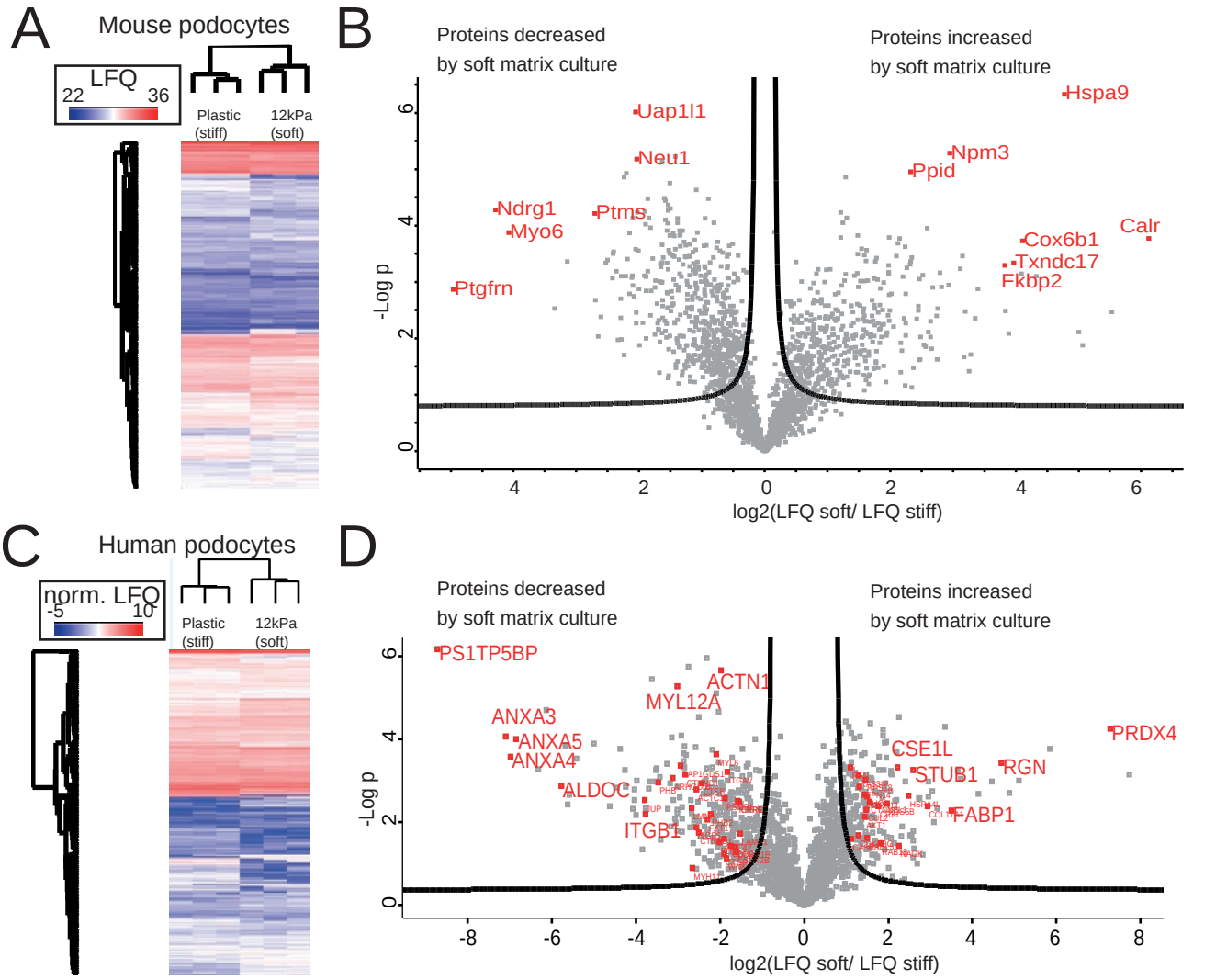
A
Mouse podocytes
LFQ
22
36
Plastic (stiff)
12kPa (soft)
B
Proteins decreased by soft matrix culture
Proteins increased by soft matrix culture
Uap1l1
Neu1
Ndrg1
Myo6
Ptms
Ptgfrn
Hspa9
Npm3
Ppid
Cox6b1
Calr
Txndc17
Fkbp2
-Log p
log2(LFQ soft/ LFQ stiff)
C
Human podocytes
norm. LFQ
-5
10
Plastic (stiff)
12kPa (soft)
D
Proteins decreased by soft matrix culture
Proteins increased by soft matrix culture
PS1TP5BP
ACTN1
MYL12A
ANXA3
ANXA5
ANXA4
ALDOC
ITGB1
CSE1L
STUB1
RGN
FABP1
PRDX4
-Log p
log2(LFQ soft/ LFQ stiff)
E
Proteins decreased with soft matrix
calcium binding
calcium-dependent phospholipid binding
cell-cell signaling
actin filament organization
cell-cell adhesion
actomyosin
actin filament bundle
stress fibers
mitochondrial inner membrane
protein-DNA complex
catenin complex
integrin complex
ENRICHMENT
F
Protein complexes decreased with soft matrix
WIPF1
MYL6
MYL12A
WAS
MYH9
ACTA2
t-test Difference_(1.500e-05
CDH2
JUP
PSEN1
CTNNB1
CDH1
t-test Difference_(9.836e-05
ITGB1
THBS1
ITGA3
t-test Difference_(1.342e-03
G
Proteins increased with soft matrix
damaged DNA binding
cellular aldehyde metabolic process
DNA-depndent DNA replicatin initiation
nucleus
cytosolic small ribosomal subunit
small ribosomal subunit
MCM complex
ENRICHMENT
H
Protein complexes increased with soft matrix
MCM7
MCMBP
MCM2
MCM3
MCM5
MCM6
MCM4
t-test Difference_(3.111e-04)
GAB1
SOS1
PTPN11
EGFR
CRK
CRKL
t-test Difference_(4.946e-02

Fig. S5

Fig. S5. Response of cultured podocytes to mechanical cues, Related to Fig. 4. A. Cultured mouse podocytes were seeded on plastic dishes (collagen coated) or on collagen coated “soft” matrix with defined elastic modulus (soft matrix, 12kPa). A proteomic profile of both groups was generated and hierarchical clustering of protein expression values was performed. B. Volcanoplot of protein quantification from podocytes on soft matrices as compared to podocytes on plastic dishes demonstrating significantly changed proteins. Proteins beyond the curved lines are significant based on FDR 0.05, s0= 0.1 C. Cultured human podocytes were seeded on plastic dishes (collagen coated) or on collagen coated “soft” matrix with defined elastic modulus (soft matrix, 12kPa). A proteomic profile was generated and hierarchical clustering of protein expression values was performed. D. Volcanoplot of protein quantification from podocytes on soft matrices as compared to podocytes on plastic dishes. E. GO-terms significantly overrepresented in proteins decreased on soft matrix. (FDR<0.05, Fishers exact test). F. Protein complexes significantly decreased on soft matrix. Protein complex enrichment analysis was performed using the COMPLEAT software for statistical overrepresentation in the dataset ($p<0.05$, corrected for multiple testing Bonferroni). G. GO-terms significantly overrepresented in proteins increased on soft matrix. (FDR<0.05, Fishers exact test). H. Protein complexes significantly decreased on soft matrix. Protein complex enrichment analysis was performed using the COMPLEAT software for statistical overrepresentation in the dataset ($p<0.05$, corrected for multiple testing).

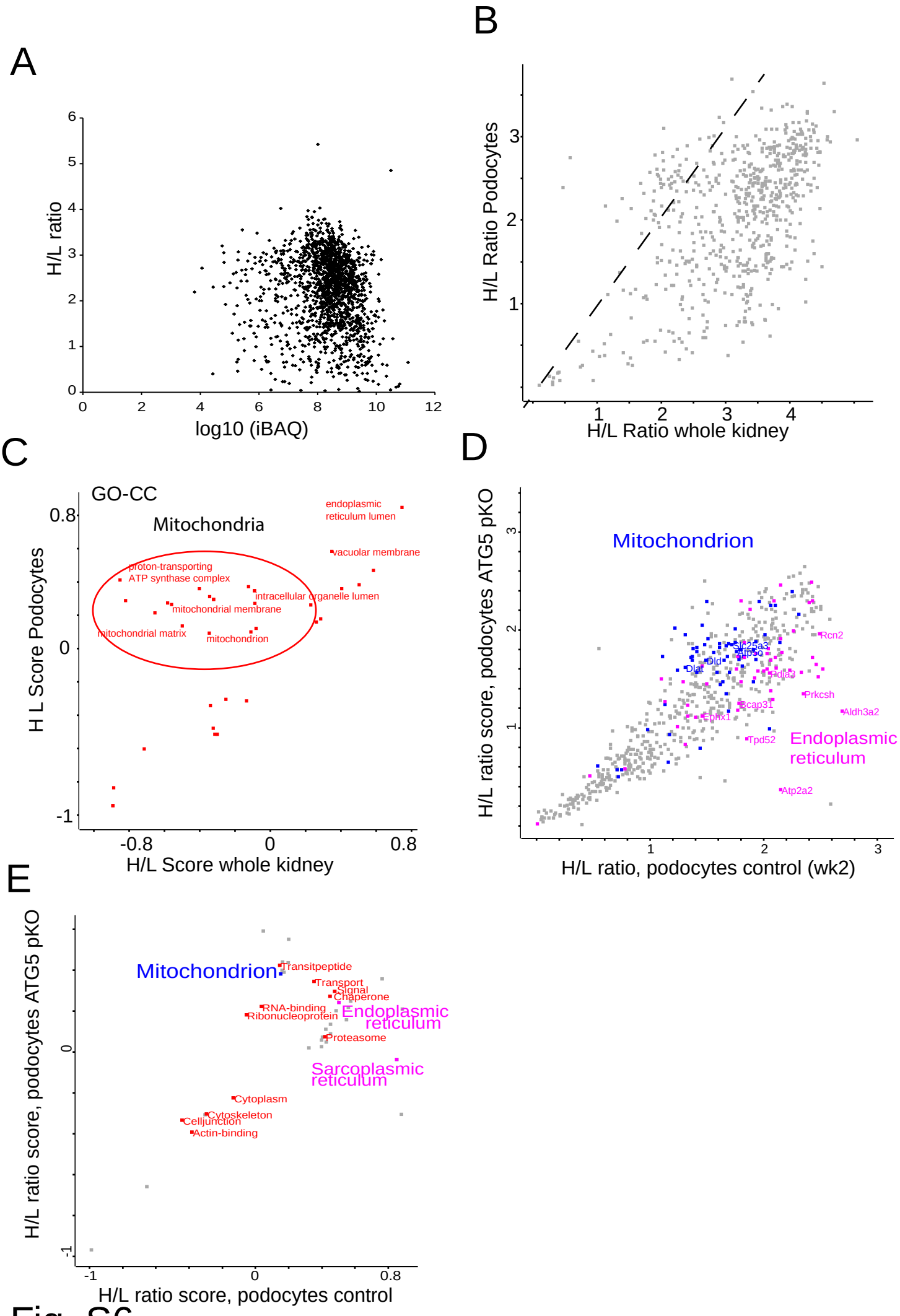
A
H/L ratio
log10 (iBAQ)
B
H/L Ratio Podocytes
H/L Ratio whole kidney
C
GO-CC
Mitochondria
endoplasmic reticulum lumen
vacuolar membrane
proton-transporting ATP synthase complex
intracellular organelle lumen
mitochondrial membrane
mitochondrial matrix
mitochondrion
H L Score Podocytes
H/L Score whole kidney
D
Mitochondrion
Endoplasmic reticulum
Rcn2
Slc25a3
Atp5o
Dld
Dlat
Pdia3
Prkcsh
Scap31
Aldh3a2
Ephx1
Tpd52
Atp2a2
H/L ratio score, podocytes ATG5 pKO
H/L ratio, podocytes control (wk2)
E
Mitochondrion
Transitpeptide
Transport
Signal
Chaperone
RNA-binding
Ribonucleoprotein
Endoplasmic reticulum
Proteasome
Sarcoplasmic reticulum
Cytoplasm
Cytoskeleton
Celljunction
Actin-binding
H/L ratio score, podocytes ATG5 pKO
H/L ratio score, podocytes control

Fig. S6

Fig. S6. Analysis of podocyte protein incorporation by pulsed in vivo stable isotope labeling, **Related to Fig. 5.** A. Scatter plot of heavy/light ratios and lg transformed iBAQ values demonstrating very weak negative correlation (R<-0.1). B. Scatter plot demonstrating H/L ratios in podocytes and whole kidney lysates. C. 2D enrichment analysis of Fig. S9B. Labeled dots determine significantly altered uniprot keyword terms (FDR < 0.05) D. Analysis of the effect of podocyte-specific ATG5 pKO on podocyte proteome as determined by pulsed stable isotope labeling in vivo. Scatterplot indicating H/L ratios in sorted podocytes of control and podocyte-specific ATG5 pKO mice after 2 weeks of feeding with stable isotope containing diet. E. 2D enrichment of Panel A (FDR<0.05). Labeled dots determine significantly altered uniprot keywords (FDR<0.05).

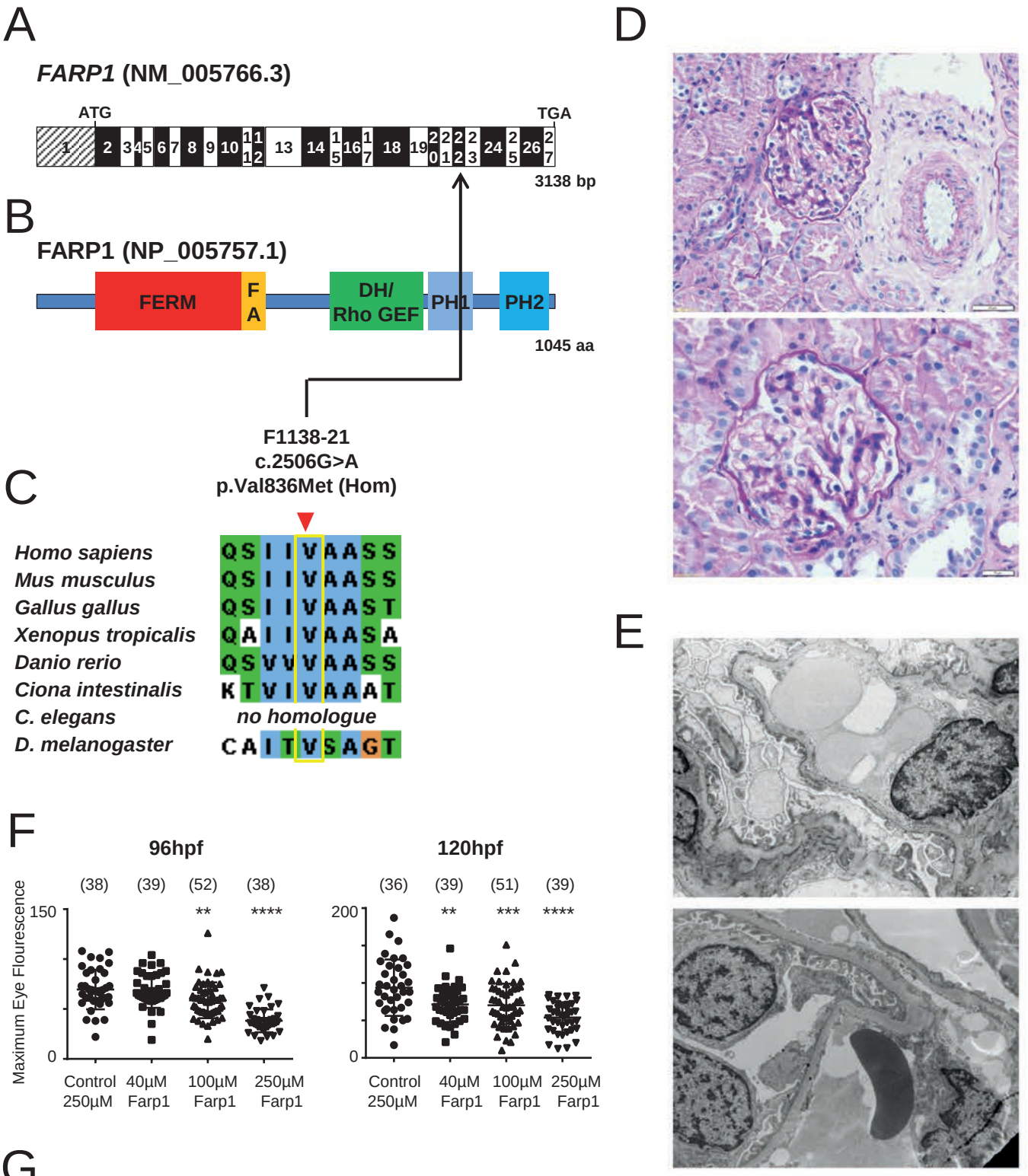
A
FARP1 (NM_005766.3)
ATG
TGA
3138 bp
B
FARP1 (NP_005757.1)
FERM
F A
DH/ Rho GEF
PH1
PH2
1045 aa
F1138-21
c.2506G>A
p.Val836Met (Hom)
C
Homo sapiens
Mus musculus
Gallus gallus
Xenopus tropicalis
Danio rerio
Ciona intestinalis
C. elegans
no homologue
D. melanogaster
D
E
F
96hpf
120hpf
Exp1
Maximum Eye Flourescence
(38) (39) (52) (38)
(36) (39) (51) (39)
Control 250μM
40μM Farp1
100μM Farp1
250μM Farp1
G
Phenotype number (%)
Phenotype severity
p1
p12
p2
p3
p4
Control 250uM
40uM Farp1
100uM Farp1
250uM Farp1

Fig. S7

Fig. S7. Whole exome sequencing identifies recessive mutations in the genes *FARP1* in a family with nephrotic syndrome, Related to Fig. 6. A. Exon structure of *FARP1* cDNA. Positions of start codon, stop codons, and mutated nucleotides are indicated. B. Domain structure of the proteins FARP1. Arrows indicate the positions of the mutated amino acid residues in families F1138 (FARP1). C. Evolutionary conservation amongst orthologous proteins of FARP1 (left). The mutated amino acid residue in family F1138 is indicated with arrowheads and a yellow box. D. Histology of renal biopsy of index patient showing focal segmental glomerulosclerosis. E. Electron microscopy of renal biopsy of index patient showing partial podocyte effacement. F. Analysis of proteinuria phenotype in zebrafish larvae. Morpholinos were injected into fertilized zebrafish eggs at one- to four-cell–stage. The transgenic zebrafish produce a vitamin D-binding protein GFP fusion protein with a size of 78kD. This protein accumulates in the circulation and is quantified 96 hpf and 120 hpf (hours past fertilization) by measuring the fluorescence level over the retina. Reduced fluorescence indicates a disturbed glomerular filtration barrier. Asterisks indicate significance in ANOVA vs control). Each dot corresponds to an individual larva, and total n numbers are depicted in brackets. G. Assessment of phenotype severity 120 hpf. The phenotype (degree of edema) was scored from P1 to P4 (with P1-2, P2 and P3 as intermediate scores, based on the amount of edema present in the yolk sac or the presence of pericardial effusion).

Supplemental Experimental Procedures

Glomerular isolation

We essentially used the same method as described previously(Boerries et al., 2013). Briefly, kidneys were dissected together with the abdominal aorta and transferred into dishes filled with 37°C prewarmed Hank's buffered salt solution (HBSS). Each kidney was perfused slowly through the renal artery with 2 ml 37°C bead solution and 0,5 ml bead solution plus enzymatic digestion buffer [containing: collagenase 300 U/ml (Worthington, Collagenase Type II, USA), 1 mg/ml pronase E (Sigma P6911, Germany) DNase I 50 U/ml (Applichem A3778, Germany)]. Kidneys were minced into 1 mm^3 pieces using a scalpel. After addition of 3 ml digestion buffer they were incubated at 37°C for 15 min on a rotator (100 rpm). The solution was pipetted up and down with a cut 1000 µl pipette tip every 5 min. After incubation all steps were performed at 4 °C or on ice. The digested kidneys were gently pressed twice through a 100 µm cellstrainer and the flow through was washed extensively with HBSS. After spin down, the supernatant was discarded and the pellet resuspended in 2 ml HBSS. These tubes were inserted into a magnetic particle concentrator and the separated glomeruli were washed twice.

Podocyte Preparation

Glomeruli were resuspended in 2 ml digestion buffer and incubated for 40 min at 37°C on a thermomixer shaking at 1400/min. During this incubation period the glomeruli were sheared with a 27 G needle at 15 min, and mixed by pipetting twice at 5, 10, 15, 20 and 25 min using a glass pipette. Podocytes were loosened at 10, 20, 30 min by vortexing once. After 40 min the solution was vortexed three times and the digestion result controlled by fluorescence microscopy. Samples were put on a magnetic particle concentrator again to eliminate beads and glomerular structures void of podocytes. The supernatant was pooled and the magnetic particles discarded. The cell suspension (2 ml) was sieved through a 40 µm pore size filter on top of a 50 ml Falcon tube, rinsed with 10 ml of HBSS. Cells were collected by centrifugation at 1500 rpm for 5 min at 4°C, resuspended in 0.5 ml of HBSS supplemented with 0.1% BSA plus DAPI (1 µg/ml). To separate GFP-expressing (GFP+) and GFP-negative (GFP-) cells, glomerular cells were sorted with a Mo-Flo cell sorter (Beckman Coulter) with a

Laser excitation at 488nm (Power 200 mW) and a sheath pressure of 60 PSI. Cells were kept at 4°C before entering the FACS machine and thereafter, while temperature during the sorting procedure (approx. 3 min) was 22°C. Only viable (DAPI negative) cells were sorted (laser excitation 380nm, power 80 mW). For the deep proteomics analysis on average 3,000,000 podocytes out of four mice (male, age 8-12 weeks) were pooled per biological replicate. For the RNASeq analysis the total RNA of nearly 12,000,000 podocytes and 19,000,000 non-podocyte glomerular cells (out of 29 mice, male, age 8-12 weeks) was used. For details on sample preparation and LC-MS/MS analysis see extended methods.

Sample preparation of podocytes for LC-MS/MS

For proteomic deep mapping, snap-frozen podocytes were dissolved in 8 M urea and 100 mM ammonium bicarbonate and lysates were generated. Protein lysates were sonicated (20 pulses, 0.1% power, 0.1s sonication cycle) and spun down at 4 degrees (16,000 g, 20min) to clear the debris. Supernatants were saved for further analysis. Protein concentration was determined using a commercial BCA assay (Thermo). 100 µg of protein were reduced with DTT (10 mM) and alkylated with iodoacetamide (40 mM) for 1h at room temperature in the dark, respectively. Podocytes were digested using trypsin at a 1:100 w/w ratio over night with shaking. The next day, ~25µg of peptides were fractionated using a six-layered SCX resin and fractionation using six different buffers as previously described: Six layered tips with SCX resin (Polystyrene-divinylbenzene copolymer modified with sulfonic acid) stage tips were conditioned with Acetonitrile (ACN) and washed with 0.2 % formic acid. Then, the supernatant was loaded on the in-tip columns and centrifuged until all of the peptide suspension passed the membrane. After washing the membrane of the stage tips with 0.2 % formic acid, 6 different cationic buffers with increasing concentrations of ammonium acetate were used to subsequently elute bound peptides: (SCX 1: 50 mM ammonium acetate (AA), 20% (v/v) ACN, 0.5% (v/v) formic acid (FA); SCX 2: 75 mM AA, 20% (v/v) ACN, 0.5% (v/v) FA; SCX 3: 125 mM AA, 20% (v/v) ACN, 0.5% (v/v) FA; SCX 4: 200 mM AA, 20% (v/v) ACN, 0.5% (v/v) FA; SCX 5: 300 mM AA, 20% (v/v) ACN, 0.5% (v/v) FA; Buffer X: 5% (v/v) Ammonium hydroxide, 80% (v/v) ACN). The flow through was collected for each of the six buffers separately during centrifugation. In the end, all the collected flow-through was dried down in a speedvac for 30 minutes at 30 °C. Subsequently peptides were stored at -20 °C until resuspension in 0.1% formic acid and subjection to nLC-MS/MS.

Bioinformatic analysis of deep proteomic data

For details on sample preparation and mass spectrometry analysis see extended methods. Raw files were analyzed using MaxQuant v 1.5.1.2 (Cox and Mann, 2008) and data was searched against a uniprot reference proteome for mouse or human downloaded at February 2014. MaxQuant options were default with match between runs enabled. The MaxQuant LFQ algorithm was enabled (Cox et al., 2014). Bioinformatic analysis was performed using Perseus v 1.5 (Cox and Mann, 2012). Briefly, reverse and contaminant hits were filtered out and proteins only identified by a site (site only) were removed. LFQ intensities were logarithmized, and a podocyte specific proteins were analyzed using a two-tailed t-test after imputation of missing values as described previously (Kohli et al., 2014). Correction for multiple testing was performed using an approach similar to SAM as initally published by Tusher et al. (Tusher et al., 2001). The parameters are detailed in the figure legends. Network analysis of podocyte-enriched proteins was performed using the netbox algorithm (Cerami et al., 2010) and default settings (p=0.05, maximal linker 2), using updated protein-protein interaction databases (3/2015) as input. The annotation of GO Terms was performed in Perseus 1.5.5.3 and a Fisher's exact test with correction for multiple testing (FDR<0.05) was utilized. The annotation of protein domains (both INTERPRO and PFAM domains) was performed in Perseus 1.5.5.3 and a Fisher's exact test with correction for multiple testing (FDR < 0.02) was performed. Enrichment was plotted vs –log (p value). mRNA seq raw values were matched on proteins using ENSEMBL identifiers, and 2D GO enrichment (FDR < 0.05) was performed. Multiple datasets were merged using ENSEMBL identifiers, and z-scored using perseus. The R package Rt-SNE was used for clustering. The raw data of the deep proteomic study is publically available via PRIDE (http://www.ebi.ac.uk/pride). PXD004040. Username: reviewer71610@ebi.ac.uk. Password: abpVHKL5. PXD005801. Username: reviewer36299@ebi.ac.uk. Password: QkntlstG.

RNA preparation and RNA sequencing

For RNA-Seq experiments isolated cells (Podocytes and Non-Podocytes glomerular cells) of 29 Gt(ROSA)$^{26Sortm4(ACTB-tdTomato,-EGFP)Luo/J}$ Tg(NPHS2-cre)295Lbh male mice at the age of 10 weeks were pooled. Under RNase-free conditions RNA was extracted with the chloroform/phenol method and DNase digested at the end of the preparation process. 15,5 µg non-podocyte and 19,2 µg podocyte

RNA were obtained. RNA quality control was performed as required by the RNASeq protocol. The Illumina (Illumina, San Diego, CA, USA) TruSeq stranded total RNA sample preparation LS protocol was used for directional, polyA+ library preparation. Sequencing was performed on a full flowcell of the HiSeq2500 sequencing machine using 100 cycles (Illumina, San Diego, CA, USA), with a depth of approximately 300M paired reads (600M total reads) and therefore approximately 150M paired reads per sample. Quality check was performed using FastQC 0.11.4 (Babraham Bioinformatics - FastQC A Quality Control tool for High Throughput Sequence Data.).

Analysis of mRNAseq data.

Pooled RNA of native mouse podocytes and non-podocytes glomerular cells was sequenced in two technical replicates. All RNA-Seq experiments were quantified using Salmon Beta 0.5.1 ((Patro et al., 2017)). RNA-Seq raw for quantification of published studies were downloaded from the European Nucleotide Archive (Toribio et al., 2017) please see Supplemental Table 3 for information about individual experiments ((Brunskill et al., 2014; Fu et al., 2016; Kann et al., 2015; Lin et al., 2014; Pervouchine et al., 2015)).

In general, analysis of transcriptomic data was performed using the R statistical software package (R Core Team (2016). R: A language and environment for statistical computing. R Foundation for Statistical Computing, Vienna, Austria. URL: https://www.R-project.org/.) as well as specific packages provided by Bioconductor (Huber et al., 2015) Graphical Plotting (Principal component, Scree plot, heat plot, histogram) was done with the help of the ggplot2 package (ggplot2 - Elegant Graphics for Data Analysis | Hadley Wickham | Springer.). Differential expression analysis was performed using sleuth version 0.28.0 using a wald test (Pimentel et al., 2017). For Reactome (Croft et al., 2014; Milacic et al., 2012) analysis ReactomePA (Yu and He, 2016) and clusterProfiler package (Yu et al., 2012) Bioconductor package was used on significantly regulated transcripts ($q < 0.001$ & $b > 1.5$) (accessed 9/2016). Raw data were deposed at EBI Array Express with experiment accession number E-MTAB-5457 (Username: Reviewer_E-MTAB-5457, Password: KC158Tch). Podocyte specificity was calculated as a ratio of tpm(Podocyte)/sum tpm (all other tissues). RNAseq datasets from other tissues were derived from the mouse RNA Profiling datasets by the ENCODE

project, using the datasets SRR453077-SRR453175; SRR567478- SRR567503, all processed in an identical fashion.

Drosophila experiments

D. melanogaster stocks were cultured on standard cornmeal molasses agar food and maintained at 25°C. RNAi-Based Nephrocyte Functional Screen Procedure: Virgins from MHC-ANF-RFP, HandGFP, and Dot-Gal4 transgenic lines (Gift from Zhe Han, University of Michigan, Ann Arbor, USA) were crossed to UAS-CG9093-RNAi (VDRC TID 9696/GD) males at 25°C; 2 days after crossing, flies were transferred to small collection cages with grape juice agar plates to collect the embryos for 24 hours at 25°C. Collected embryos were aged for 48 hours at 29° C and then subjected to examination of the RFP accumulation in pericardial nephrocytes using a confocal microscope. The RFP mean fluorescence intensity of GFP positive areas was measured to quantify the uptake efficiency. The result was verified using a second RNAi (VDRC 101473/KK). For transmission electron microscopy Virgins of prospero-Gal4 (gift from Barry Denholm, University of Edinburgh, Edinburgh, UK) were crossed to UAS-CG9093-RNAi (VDRC TID 9696/GD) for a garland cell-specific knockdown of Tsp26A. Drosophila garland cells were freshly prepared and immerse fixed for three days at 4°C using 4% paraformaldehyde plus 1% glutaraldehyde (Sigma Aldrich, Germany; in 0.1M PB buffer, pH 7.4) as a fixative. The samples were contrasted using 1% osmiumtetroxide (Roth, Germany; 30 min at RT) and 1% uranylacetate (30 min at RT in 70% ethanol), dehydrated stepwise and finally embedded in epoxy resin (Durcopan, SimgaAldrich, Germany). Ultrathin sections were cut using a Leica Ultracut 6. Section imaging and analysis was performed using a Philipps CM10 TEM.

Sample preparation for proteomic analysis of cell culture experiments.

Cells were harvested by scraping in 8M urea and 100mM Ammonium bicarbonate on ice with 1x protease/phosphatase inhibitor. Then, proteins were reduced (5 mM DTT at room temperature for 1h), and alkylated (10mM IAA at room temperature for 1h in the dark). The proteins (~50 µg as determined by a BCA assay [Thermo]) were digested using a 1:100 trypsin/protein ratio over night at room temperature. The next day, peptide solution was acidified and subjected to Stage tip cleanup as

above described (Rappsilber et al., 2003) and mass spectrometry analysis on a Q Exactive plus machine as previously described (2.5 h gradient). For details on bioinformatics analysis, please see supplementary methods.

Bioinformatic analysis of cell culture experiments

Raw data was processed with MaxQuant and intensities were logarithmized, contaminants were removed and raw data was normalized by substraction of the mean. Data were uploaded in perseus and hierarchical clustering (based on Euclidean distance) was performed. Imputation was performed for at least 4/6 valid values. COMPLEAT (Vinayagam et al., 2013) algorithm was utilized to determine regulated protein complexes in human podocytes. The log2 ratio of LFQ (con/12kPA) was utilized as software input with default settings (accessed 12/2016). GO terms and uniprot keywords were annotated in perseus (v. 1.5.5.3) (Tyanova et al., 2016) and category enrichment was performed by a Fisher's exact test (FDR controlled with FDR <0.05). Data was extracted from the human protein atlas in February 2015 and converted into mouse gene symbols using NCBI homologene groups (release 3/2015), which were then matched on the dataset.

Pulsed in vivo stable isotope labeling

Stable isotope labeling of animals was performed as previously described by Krueger et al. (Krüger et al., 2008) Lys(0)-SILAC-Mouse control ($^{12}C_6$-lysine) and Lys(6)-SILAC-Mouse SILAC ($^{13}C_6$-lysine, 97 %) mouse diet was purchased from Silantes, Martinsried, Germany. Mice in SILAC feeding experiments were kept isolated in single individual cages with metal grids. Initially Mice were fed 3 g daily of Lys(0)-SILAC-Mouse control diet for 3 weeks. Afterwards they were switched to 3 g daily Lys(6)-SILAC-Mouse SILAC diet for 1, 2 or 3 weeks according to the experimental protocol and sacrificed afterwards for glomerular isolation. Please see Supplemental table 14+15 for additional details of mice used for this study. The data presented are the average of at least 2 biological replicates for podocytes (for three different timepoints) and kidney tissue.

Sample preparation and proteomics of in vivo stable isotope labeled tissue

SILAC mice and kidneys were perfused and podocytes were isolated exactly as described above. Then, snap-frozen podocytes were lysed in SDS and fractionated using 1D Gel electrophoresis and processed as previously described in gel-with 6-10 gel pieces/protein (Boerries et al., 2013). The digestion was performed with LysC (w/w ratio of 1:10). Analysis of pulsed SILAC labeled podocytes was performed using an LTQ Orbitrap XL mass spectrometer coupled to a nLC as previously described (Boerries et al., 2013).

Bioinformatic analysis of dynamic proteomic data

Proteomics data were searched with MaxQuant v 1.4.1.2 against an UNIPROT mus musculus database downloaded on March 2016. Multiplicity was set to 2 (with Lysine + 6 Da), and the maximal number of labeled amino acids was 4. The protease was LysC/P, with three maximal missed cleavages. Minimum peptide length was 7, variable modifications were methionine oxidation and protein N-terminal acetylation. Carbamidomethylcysteine was set as fixed modification. MatchBetweenRun option was not enabled. The non-normalized ratios were used for further procedures. The resulting ratios were merged using Perseus und filtered for reverse, contaminant and "site only" proteins Then, the resulting matrix was filtered so only valid ratios were obtained. 2D GO enrichment analyses were applied as described above. H/L ratios were normalized using the following term depicting the "number of heavy amino acids", using the iBAQ obtained from Fig. 1 and using the amino acid copy numbers obtained from uniprot for the leading majority protein. The following formula was used to correct ratios:

$$n(heavy\ amino\ acids) = incorporation\ rate * n(amino\ acids\ per\ protein) * n(protein\ copies)$$

$$= \frac{H/L}{H/L + 1} * n\ (amino\ acids\ per\ protein) * iBAQ$$

In situ hybridization

Mouse isolated podocyte RNA served to clone fragments of 5′-UTR and coding sequence of mouse *Farp1* using the One-Step PCR Kit (Qiagen, Heidenheim, Germany). PCR fragments were

inserted into a modified *pBluescript (KS-)* vector (Invitrogen, Carlsbad, CA) using *NotI* and *MluI* restriction sites. *pBluescript* Vector was linearized and digoxigenin-(DIG)-labeled antisense riboprobes were generated using T7-RNA-polymerase (Roche, Mannheim, Germany). For paraffin section ISH, slides were progressively rehydrated. After prehybridization (20 min), hybridization with DIG-UTP probes took place overnight in standard hybridization buffer (SSC pH 4.5; containing deionized 50% formamide, 1% SDS, heparine 50µg/ml and yeast RNA 50µg/ml) at 60 °C. Specimens were then incubated with alkaline phosphatase-conjugated anti-DIG Fab fragments (Roche, Mannheim, Germany) at a dilution of 1:3000 for 2 h at room temperature. Alkaline phosphatase was detected using chromogenic conversion of BM Purple (Roche). Slides were then progressively dehydrated in xylol, counterstained with Eosin and mounted. The following primers were used:

Farp1(based on NM_028734.5)

ISH FARP1 449 fp 5'-CGCGGGACGCGTTGGAACGAGGACAGAAACCA -3'

ISH FARP1 1445 rp 5'- CGCGGGGCGGCCGCTTGTGGCCGCCTTCTTTAAC-3';

Multi-omics candidate gene list, whole exome sequencing, multi gene-panel testing and mutation calling.

To obtain a candidate list of genes we performed clustering analysis of z-normalized relative mRNA expression levels, relative protein expression levels, absolute protein expression levels as well as tissue specificity of the podocyte mRNA levels. We found that disease-associated genes in slit diaphragm and actin-related processes were largely defined by very high z-scores in all four parameters, and clustered in close proximity. Ranking individual genes based on their scores in each parameter, combined with additional information from the human protein atlas, glomerular disease datasets (www.nephromine.org), as well as importance of the respective gene in go-term analysis generated a list of 280 candidate gene-protein pairs. To test these in patient cohorts, we performed different next-generation sequencing (NGS) based approaches. First, we performed whole exome sequencing (WES) using Agilent SureSelect™ human exome capture arrays (Thermo Fisher Scientific) with NGS on an Illumina™ platform. Sequence reads were mapped against the human reference genome (NCBI build 37/hg19) using CLC Genomics Workbench (version 6.5.1) (CLC bio).

Mutation calling was performed in line with proposed guidelines by scientists, who had knowledge of clinical phenotypes, pedigree structure, and genetic mapping. 430 families with nephrotic syndrome were screened for mutations in 280 candidate genes derived from the “multi-omics” approach. Families with mutations in genes known to cause nephrotic syndrome, if mutated, were excluded from the study. Second, all exons and adjacent intronic boundaries of a different number of genes (dependent on the version of our customized multi-gene panel, including *FARP1*) known or hypothesized to cause nephrotic syndrome and related phenotypes were targeted by a custom SeqCap EZ choice sequence capture library (NimbleGen, Madison, Wisconsin, USA) and subsequently sequenced on an Illumina MiSeq or HiSeq platform (2x150 PE) according to the manufacturer´s protocol. A total of 700 patients were analyzed with an average coverage of 120-fold (MiSeq) or more than 200-fold (HiSeq), respectively. Bioinformatic analysis was performed as recently described.

Zebrafish experiments

Transgenic zebrafish Tg(l-fabp:DBP-EGFP) were a kind gift from B. Anand-Apte, Cleveland, OH (Xie et al., 2010). They were grown and mated at 28.5° C and embryos were kept and handled in standard E3 solution as previously described (Hentschel et al., 2007). Morpholino sequence for farp1 was 5'UTR: GTGTCTTTAAATGATATTCCGCTGG, for control: CCTCTTACCTCAGTTACAATTTATA. They were injected in one- to four-stage embryos using a Nanoject II injection device (Drummond Scientific, Broomall, PA). Morpholinos were ordered from GeneTools (Philomath, OR). Injections were carried out in injection buffer (100 mM KCl, 0.1% phenol red) and at 48 hours post fertilization (hpf) remaining chorions were manually removed. Edema assessment and fluorescence based eye assays were performed as previuously described (Hanke et al., 2013). The animal protocol was approved by the MDI Biological Laboratory IACUC (#11-02).

Supplemental References

Bartram, M.P., Habbig, S., Pahmeyer, C., Höhne, M., Weber, L.T., Thiele, H., Altmüller, J., Kottoor, N., Wenzel, A., Krueger, M., et al. (2016). Three-layered proteomic characterization of a novel ACTN4 mutation unravels its pathogenic potential in FSGS. Hum. Mol. Genet.

Boerries, M., Grahammer, F., Eiselein, S., Buck, M., Meyer, C., Goedel, M., Bechtel, W., Zschiedrich, S., Pfeifer, D., Laloë, D., et al. (2013). Molecular fingerprinting of the podocyte reveals novel gene and protein regulatory networks. Kidney Int. *83*, 1052–1064.

Brunskill, E.W., Park, J.-S., Chung, E., Chen, F., Magella, B., and Potter, S.S. (2014). Single cell dissection of early kidney development: multilineage priming. Dev. Camb. Engl. *141*, 3093–3101.

Croft, D., Mundo, A.F., Haw, R., Milacic, M., Weiser, J., Wu, G., Caudy, M., Garapati, P., Gillespie, M., Kamdar, M.R., et al. (2014). The Reactome pathway knowledgebase. Nucleic Acids Res. *42*, D472-477.

Fu, J., Wei, C., Lee, K., Zhang, W., He, W., Chuang, P., Liu, Z., and He, J.C. (2016). Comparison of Glomerular and Podocyte mRNA Profiles in Streptozotocin-Induced Diabetes. J. Am. Soc. Nephrol. JASN *27*, 1006–1014.

Hanke, N., Staggs, L., Schroder, P., Litteral, J., Fleig, S., Kaufeld, J., Pauli, C., Haller, H., and Schiffer, M. (2013). “Zebrafishing” for novel genes relevant to the glomerular filtration barrier. BioMed Res. Int. *2013*, 658270.

Hentschel, D.M., Mengel, M., Boehme, L., Liebsch, F., Albertin, C., Bonventre, J.V., Haller, H., and Schiffer, M. (2007). Rapid screening of glomerular slit diaphragm integrity in larval zebrafish. Am. J. Physiol. Renal Physiol. *293*, F1746-1750.

Huber, W., Carey, V.J., Gentleman, R., Anders, S., Carlson, M., Carvalho, B.S., Bravo, H.C., Davis, S., Gatto, L., Girke, T., et al. (2015). Orchestrating high-throughput genomic analysis with Bioconductor. Nat. Methods *12*, 115–121.

Kann, M., Ettou, S., Jung, Y.L., Lenz, M.O., Taglienti, M.E., Park, P.J., Schermer, B., Benzing, T., and Kreidberg, J.A. (2015). Genome-Wide Analysis of Wilms’ Tumor 1-Controlled Gene Expression in Podocytes Reveals Key Regulatory Mechanisms. J. Am. Soc. Nephrol. JASN *26*, 2097–2104.

Krüger, M., Moser, M., Ussar, S., Thievessen, I., Luber, C.A., Forner, F., Schmidt, S., Zanivan, S., Fässler, R., and Mann, M. (2008). SILAC mouse for quantitative proteomics uncovers kindlin-3 as an essential factor for red blood cell function. Cell *134*, 353–364.

Lin, S., Lin, Y., Nery, J.R., Urich, M.A., Breschi, A., Davis, C.A., Dobin, A., Zaleski, C., Beer, M.A., Chapman, W.C., et al. (2014). Comparison of the transcriptional landscapes between human and mouse tissues. Proc. Natl. Acad. Sci. U. S. A. *111*, 17224–17229.

Milacic, M., Haw, R., Rothfels, K., Wu, G., Croft, D., Hermjakob, H., D’Eustachio, P., and Stein, L. (2012). Annotating cancer variants and anti-cancer therapeutics in reactome. Cancers *4*, 1180–1211.

Patro, R., Duggal, G., Love, M.I., Irizarry, R.A., and Kingsford, C. (2017). Salmon provides fast and bias-aware quantification of transcript expression. Nat. Methods *14*, 417–419.

Pervouchine, D.D., Djebali, S., Breschi, A., Davis, C.A., Barja, P.P., Dobin, A., Tanzer, A., Lagarde, J., Zaleski, C., See, L.-H., et al. (2015). Enhanced transcriptome maps from multiple mouse tissues reveal evolutionary constraint in gene expression. Nat. Commun. *6*, 5903.

Pimentel, H., Bray, N.L., Puente, S., Melsted, P., and Pachter, L. (2017). Differential analysis of RNA-seq incorporating quantification uncertainty. Nat. Methods *14*, 687–690.

Toribio, A.L., Alako, B., Amid, C., Cerdeño-Tarrága, A., Clarke, L., Cleland, I., Fairley, S., Gibson, R., Goodgame, N., Ten Hoopen, P., et al. (2017). European Nucleotide Archive in 2016. Nucleic Acids Res. *45*, D32–D36.

Xie, J., Farage, E., Sugimoto, M., and Anand-Apte, B. (2010). A novel transgenic zebrafish model for blood-brain and blood-retinal barrier development. BMC Dev. Biol. *10*, 76.

Yu, G., and He, Q.-Y. (2016). ReactomePA: an R/Bioconductor package for reactome pathway analysis and visualization. Mol. Biosyst. *12*, 477–479.

Yu, G., Wang, L.-G., Han, Y., and He, Q.-Y. (2012). clusterProfiler: an R package for comparing biological themes among gene clusters. Omics J. Integr. Biol. *16*, 284–287.

Babraham Bioinformatics - FastQC A Quality Control tool for High Throughput Sequence Data.

ggplot2 - Elegant Graphics for Data Analysis | Hadley Wickham | Springer.